Available online at www.sciencedirect.com
ScienceDirect
Polymer 47 (2006) 7355–7360
polymer
www.elsevier.com/locate/polymer

Microscale analysis of patterning reactions via FTIR imaging: Application to intelligent hydrogel systems

Dipti Biswal, J. Zach Hilt*

Department of Chemical and Materials Engineering, University of Kentucky, 177 F. Paul Anderson Tower, Lexington, KY 40506-0046, USA

Received 27 June 2006; received in revised form 7 August 2006; accepted 9 August 2006
Available online 7 September 2006

Abstract

A novel application of FTIR imaging for real-time characterization of patterning polymerization processes with microscale spatial resolution is presented. These methods will enable the microscale analysis of the reactions of polymeric systems with various substrates and devices. Specifically, intelligent hydrogels containing ionic groups (pH responsive) and poly(ethylene glycol) have been micropatterned onto gold surfaces, and the free-radical polymerization reaction has been characterized. It was demonstrated that differences in the reaction rates across a patterned region could be successfully resolved and characterized. This novel characterization method based on FTIR imaging will facilitate the optimization of integration processes of patterned polymeric films leading to enhanced (and reproducible) application of these materials as functional components in a variety of microdevices.
© 2006 Elsevier Ltd. All rights reserved.

Keywords: FTIR imaging; Hydrogel; Microcontact printing

1. Introduction

Hydrogel systems have immense potential as functional components in micro- and nanoscale applications, especially in the biological and medical fields [1]. Some recent examples of the use of these biomaterials in micro- and nanodevices include the integration of responsive hydrogels with silicon microcantilevers for application as bioMEMS sensors [2,3] and in microfluidic channels for valve applications [4,5]. For these and similar applications to be realized, the ability to synthesize and characterize the hydrogel structures at the micro- and nanoscale is critical, and currently there are limited methods available for micro- and nanoscale characterization of hydrogel structures. In this work, the first demonstration and application of a method for real-time characterization of patterning polymerization processes with microscale spatial resolution is presented. This novel method will enable the microscale control and optimization of processes for the integration of polymeric systems with silicon, glass, and gold surfaces in devices. The ability to optimize the integration of these polymers is critical for the fabrication and development of platforms that harness the unique abilities of intelligent polymer networks, including diagnostic devices, therapeutic devices, tissue engineering, microarray, and diagnostic and therapeutic clinic-on-a-chip.

Hydrogels are mainly hydrophilic polymer networks that swell to a high degree in water or biological fluids due to an extremely high affinity for water, yet are insoluble because of the incorporation of chemical or physical crosslinks. Typically, these systems have good biocompatibility leading to widespread application as biomaterials, such as in contact lenses, sutures, dental materials, and controlled drug delivery devices. By tailoring their molecular structure and functionality, polymer networks can be created that interact with their environment in a pre-programmed, intelligent manner. Intelligent polymer networks have been created based on a variety of polymer systems, including environmentally responsive hydrogels, biohybrid hydrogel networks, and configurationally biomimetic imprinted polymers [6–10].

Conventional FTIR microscopy has been around for many years and proven to be a valuable research tool, yet it has

* Corresponding author. Tel.: +1 859 257 9844; fax: +1 859 323 1929.
E-mail address: hilt@engr.uky.edu (J.Z. Hilt).

0032-3861/$ - see front matter © 2006 Elsevier Ltd. All rights reserved.
doi:10.1016/j.polymer.2006.08.028

limitations due to its single point analysis and long acquisition times [11]. Since first being developed a decade ago [12], FTIR microscopes equipped with a focal plane array (FPA) detector have become the start-of-the-art in FTIR imaging [13]. The FPA detector consists of an array of detectors that simultaneously capture the interferometer signal, allowing for a spatial resolution (pixel size) of approximately 5.5 μm. Since its development, FTIR imaging has been utilized in a wide variety of applications, where it is advantageous to acquire chemical information with microscale resolution. For example, it has been applied for high-throughput analysis of the material properties of pharmaceutical formulations [11]. Several other researchers have utilized FTIR imaging to examine drug release processes [14–16], polymer dissolution [17,18], and it has also been applied for histopathologic recognition [19]. Although post-reaction FTIR imaging studies have been performed to examine conversions of micropatterning polymerizations [20], there have not been any *in situ* studies to spatially resolve the kinetics of micropatterning reactions. In the following, reaction kinetics are spatially resolved in real-time with FTIR imaging allowing for an extra dimension of analysis and, thus, control of the integration process.

2. Experimental section

2.1. Materials

Methacrylic acid (MAA) and tetraethylene glycol dimethacrylate (TEGDMA) were purchased from Polyscience Inc., (Warrington, PA). The initiator 2,2′-azobisisobutyronitrile (AIBN) and 1-octadecanethiol were purchased from Aldrich Chemical Company (Milwaukee, WI). The silicon and gold wafers used in this process were obtained from Virginia Semiconductor Inc. (Fredericksburg, VA) and Platypus Technologies (Madison, WI), respectively. SU-8, an epoxy based negative photoresist, was purchased from MicroChem Corp. (Newton, MA). Sylgard 184, a precursor solution for polydimethylsiloxane (PDMS), was donated by Dow Corning (Midland, Michigan). Methacrylic acid was used after vacuum distillation, and all other chemicals were used as received.

2.2. Micropatterning reaction methodology

2.2.1. Preparation of master chips and PDMS stamp

The patterned master chips used for microcontact printing (μCP) were prepared by UV photolithography. First, Si wafers were sonicated in acetone for 1 min and washed with Millipore water and dried in a steam of nitrogen. The wafer was then baked on a hotplate at 100 °C for 2 min in order to dehydrate the surface. A 25 μm film of SU-8 was spin coated onto the wafer using a spin speed of 2000 rpm for 45 s. The film of the photoresist was soft-baked on a hotplate (65 °C, 3 min; 95 °C, 7 min) to evaporate the solvent. Patterns of squares were produced in the hardened film by exposure to UV light (Karl Suss MJB3 Mask Aligner). The post-exposure bake (65 °C, 1 min; 95 °C, 3 min) was performed on a hotplate, selectively crosslinking the exposed regions of photoresist. The unexposed portions were then removed by immersion of the substrate in SU-8 developer (4 min) followed by rinsing in isopropanol and drying in a steam of nitrogen.

For the microscale control over the patterning reactions, soft lithography techniques were employed. After fabrication of the master chips, the microstamp was prepared using PDMS. The micropatterned master chip was replicated with Sylgard 184 using a PDMS base-to-crosslinker ratio of 10:1. The base and the cure agent were mixed in a small beaker followed by sonication for 5 min in order to remove the air bubbles. The silicon chip was put on the solid sheet of a magnet and then another sheet of magnet with a circular geometry cut from the center was put on the top. Then desired amount of the sonicated PDMS was pipetted into the mold, being careful to avoid trapping air in the mold. The PDMS stamp was cured at 100 °C for 1 h. Finally, the cured PDMS stamp was easily separated from the magnet sheet.

2.2.2. Preparation of self-assembled monolayers (SAMs)

The PDMS microstamps were utilized to spatially control the polymerization reaction, and a schematic of the experimental procedure is included in Fig. 1. First, gold-coated silicon

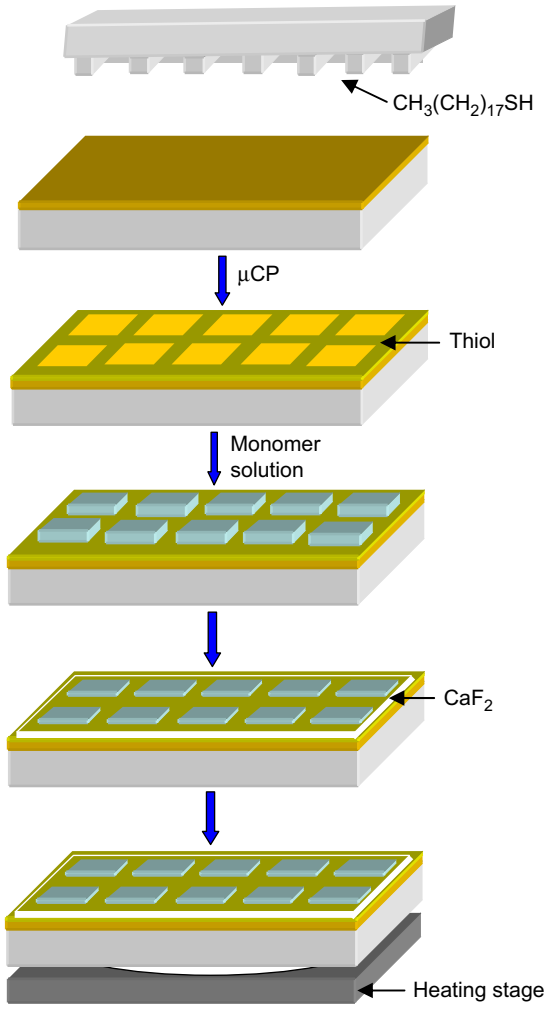

Fig. 1. A schematic diagram of pattern thiol monolayer formation and reaction setup.

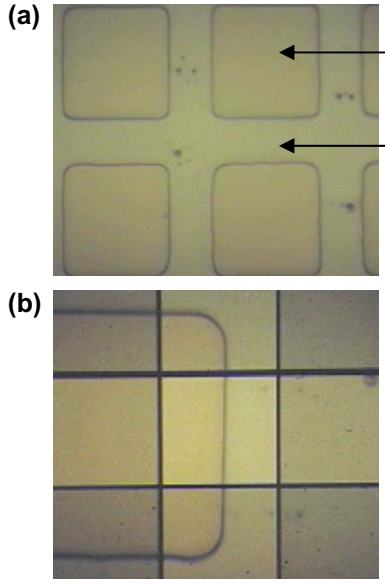

Fig. 2. Formation of pattern SAM: (a) visible image of pattern squares with monomer solutions and (b) a visible image of a focused square.

wafers were patterned with self-assembled monolayers (SAMs) using μCP techniques. The gold substrate obtained from Platypus Technologies, was an electron beam deposited gold film (ca. 1000 Å) over titanium layer on silicon wafer. In brief, the PDMS stamp was inked by a few drops of 1 mM solution of 1-octadecanethiol in ethanol and blown in dry air for 10 s, and then, the PDMS stamp was brought in contact with a freshly cleaned gold wafer for 30 s. The gold surface modified with SAMs was rinsed subsequently with ethanol, water, and then dried.

2.3. Polymerization and FTIR imaging

The polymerization reaction between methacrylic acid (MAA) and tetraethylene glycol dimethacrylate (TEGDMA) crosslinker was carried out using 2,2′-azobisisobutyronitrile (AIBN) to initiate a free-radical polymerization. Specifically, a monomer mixture with 80:20 mol% of MAA and TEGDMA was prepared with 1 wt% AIBN initiator. The monomer solution was then applied to the microstamped gold surface. In order to limit oxygen inhibition of planar diffusion during polymerization the solution was covered with a 2 mm thick CaF_2 window. The reaction assembly was then placed onto FTIR microscope heating stage. A schematic diagram of the above procedure is shown in Fig. 1. As a result of the μCP of the hydrophobic thiols, the monomer solutions remained only on the square zones that were unmodified by stamping (Fig. 2a). These hydrophilic/hydrophobic interactions successfully created the micropattern regions containing hydrophilic monomer solution or hydrophobic thiol (air). Then, a thermal-initiated polymerization reaction (60 °C) was carried out on the FTIR microscope stage to create micropatterned hydrogel structures. All spectra and FTIR images were collected by a Digilab Stingray system consisting of FTIR 7000e step-scan spectrometer (Varian Inc.) and UMA 600 IR microscope. The imaging detector used is an FPA consisting of a 16×16 array of mercury cadmium telluride (MCT) elements, covering a sample area of 88×88 μm^2. Spectra were measured with 8 cm^{-1} spectral resolution and within the range of 4000–900 cm^{-1}. Sixteen scans co-addition were used, and the total acquisition time was approximately 25 s. All the scans were taken in the reflection mode.

3. Results and discussion

On heating, the free-radical polymerization is initiated, and as the reaction proceeds, the C=C of the monomers gradually disappear. To visualize the kinetics of the patterning reaction via FTIR imaging, the edges of the square patterns were focused on facilitating the simultaneous analysis of reacting and un-reacting zones (Fig. 2b). Scans at different time intervals were carried out for the same focused position. Data for spectra corresponding to the spectroscopic information stored in a single pixel in the reacting zone were obtained at different time intervals and included in Fig. 3. From Fig. 4 it has been clearly observed that with the increase in the reaction time the

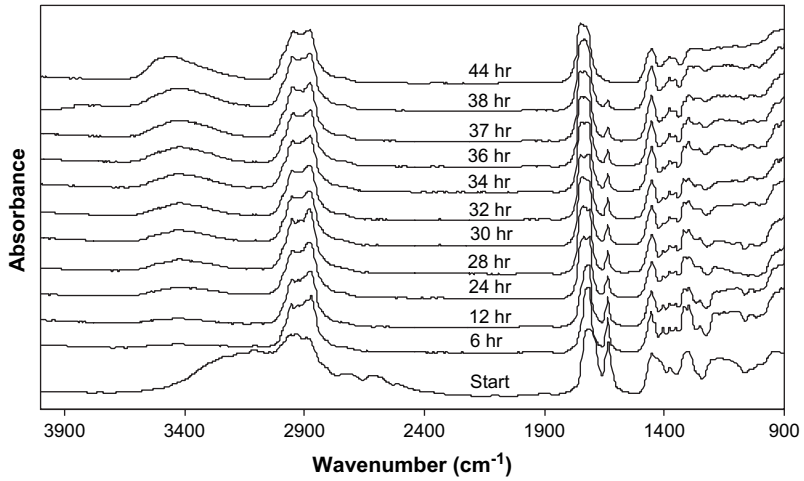

Fig. 3. FTIR spectra from the same pixel at different reaction times showing the decrease in C=C absorbance with time.

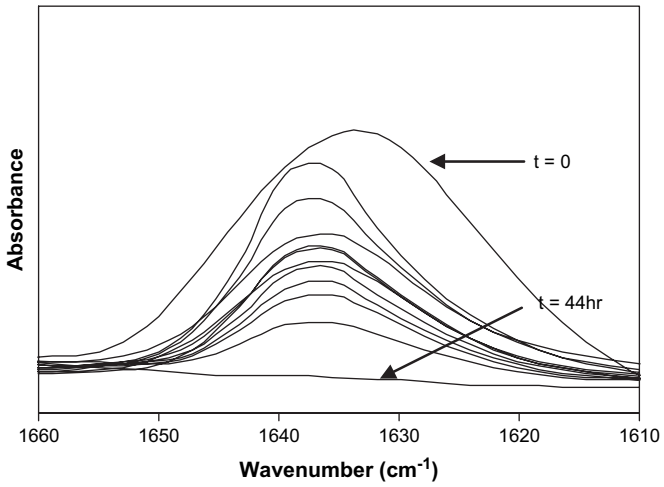

Fig. 4. IR spectra at 1636 cm^{-1} showing the decrease in peak area with reaction time.

absorbance (peak area) at 1636 cm^{-1} due to C=C vibration also decreased and eventually disappeared. As the reaction proceeded, a new peak appeared at 3430 cm^{-1} which may be due to the possible intermolecular or intramolecular hydrogen bonding between the carboxylic groups or between carboxylic group and the oxygen groups in TEGDMA [21,22].

FTIR images, where the area of the 1636 cm^{-1} peak is plotted as a color gradient, were captured at different interval of times during the reaction. The reduction of C=C absorbance peak area with time is clearly visualized in Fig. 5. Also, 3D-images of the same data at selected time intervals are included in Fig. 6. These images demonstrate the spatial resolution of the polymerization reaction.

The polymerization only occurs within the square patterns on the gold wafer, and the reaction is expected to be inhibited by oxygen diffusion and inhibition (radical scavenging) near the monomer/air interface. To observe this effect, points (A–D) inside and outside of the square reacting zone were selected and analyzed at various extents of reaction (Fig. 7a). Since no monomer is present at point D, there was no significant C=C absorbance at that location (Fig. 7b).

The conversion of the monomers, for each spectrum at the points A–C, was determined by standard baseline techniques using the peak area of the 1636 cm^{-1} for C=C vibration and the area of 1713 cm^{-1} for C=O stretching as reference. The conversion of the double bond was determined from the following formula:

$$\xi = 1 - \frac{c_t}{u} \tag{1}$$

where c_t is the ratio of peak area of the C=C to the reference peak area of C=O at time t, and u is the ratio of same peak area at $t = 0$. From Fig. 8, the conversion versus time curves, it has been clearly observed that at a particular time the rate of conversion at point A was highest followed by B and C. The rate of conversions for points A–C gradually increased with time due to autoacceleration or gel effect [23]. As the degree of polymerization became high, the viscosity has been increased. After a particular point the polymer molecules that reached a certain chain length became entangled with the other polymer

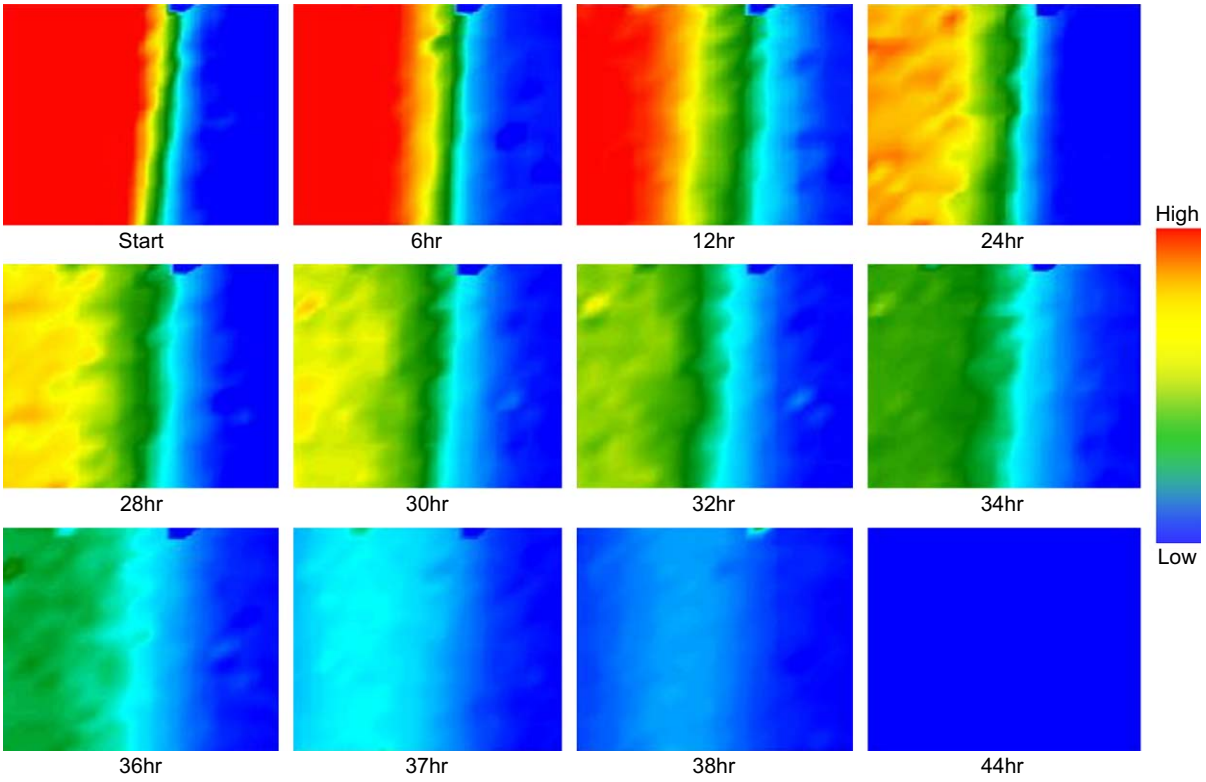

Fig. 5. FTIR images of spectral slices extracted from 1636 cm^{-1} as a function of reaction time. Scale bars indicate highest and lowest intensities, respectively.

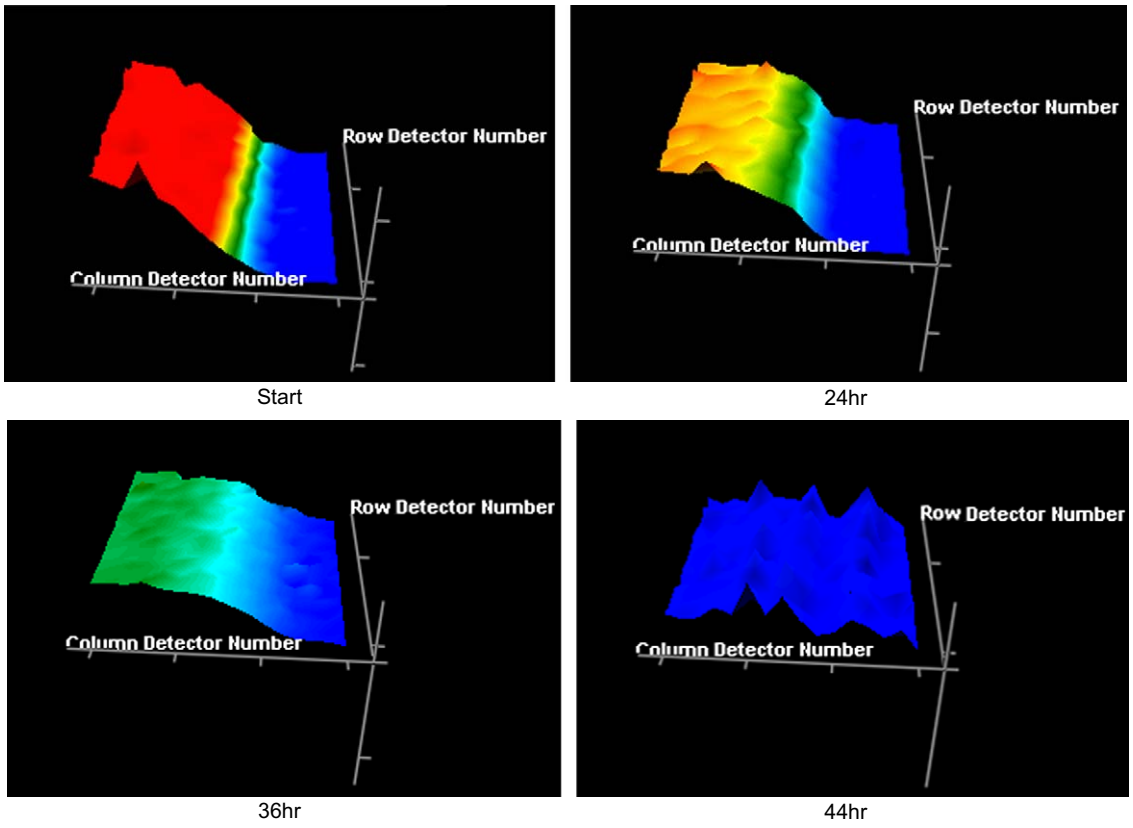

Fig. 6. 3-D images at different time intervals showing the decrease in intensities with time.

molecules. Therefore, the mobility of these molecules or the chain lengths of the active sites severely reduced. Because of this reduction in mobility, the probability of two polymer chains reacting with each other becomes much lower, reducing the magnitude of the termination rate constant.

The curing rates ($d\xi/dt$) were determined from the derivatives of the conversion curves. It has been observed from Fig. 9 that the rate of the reaction at point A is higher than B and C, and, thus, the closer to the monomer/air interface, the slower the rate of the reaction. As the viscosity increases, the diffusion-limited termination reactions are slowed, increasing the overall rate of reaction, even though the rate constant of the propagation step is unaffected. As the concentration of polymer molecules increased, the rate of diffusion has been dropped dramatically for both the polymer chains to diffuse together. The rate of termination decreases because the polymer chains entangle, but monomers can diffuse through the chains to maintain propagation.

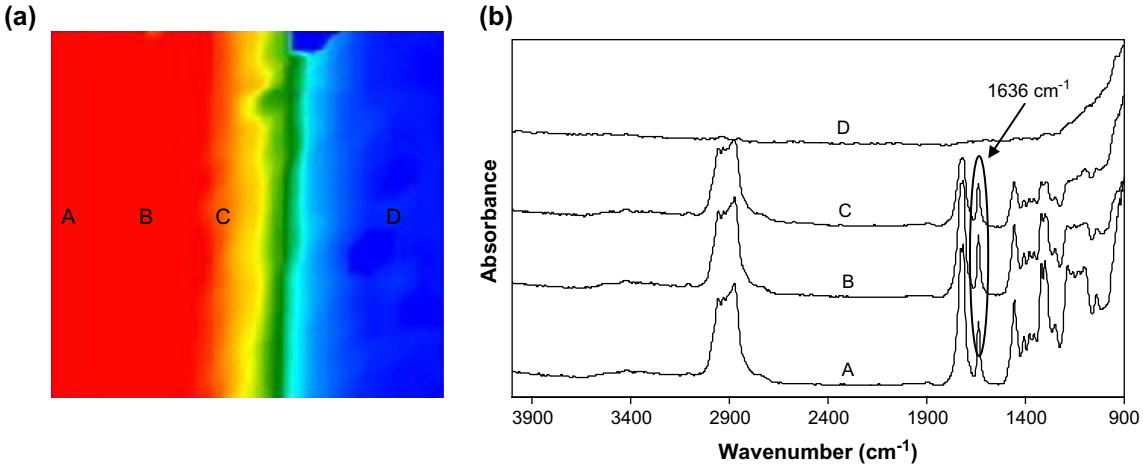

Fig. 7. Spatial analysis of the reaction kinetics. (a) FTIR image showing the points where the polymerization kinetics were analyzed and (b) spectra at the points A–D showing the absorbance at a particular reaction time.

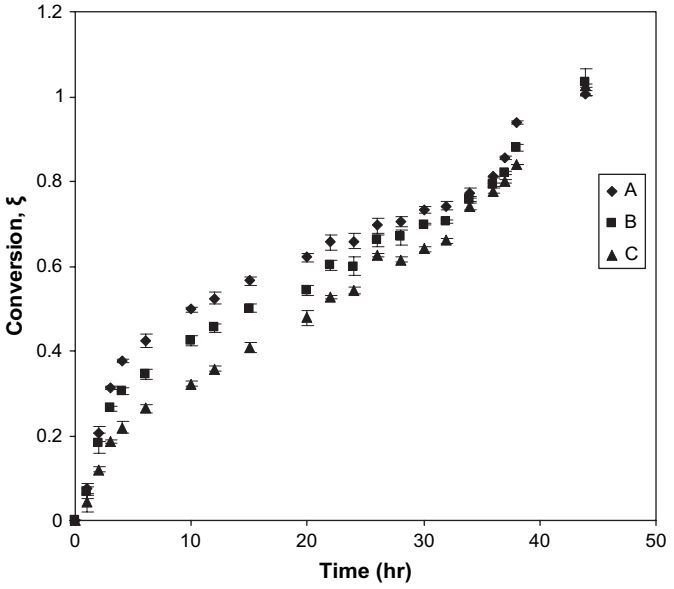

Fig. 8. Plot of conversion versus time for the points A–C at different time intervals shows the lower conversion near the interface.

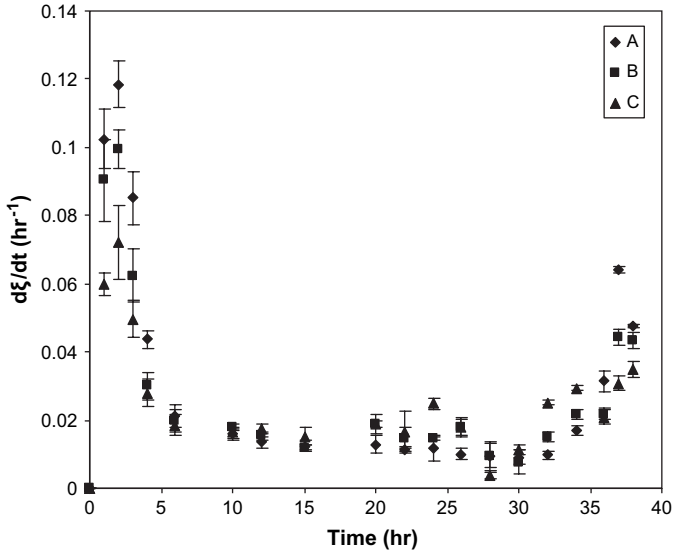

Fig. 9. Curing rates versus time curves determined from the derivatives of conversion curves show the higher rate of polymerization at point A, followed by B and C.

4. Conclusions

Spectrochemical imaging is a powerful and information rich technique applicable to a variety of disciplines and applications. FTIR imaging is successfully applied for *in situ* studies to spatially resolve the kinetics of micropatterning reaction. Our studies demonstrate for the first time a method for the real-time characterization of patterning polymerization processes with microscale spatial resolution. This enables for the spatial analysis of the polymeric reactions as they proceed in ''real time'', resulting in an additional dimension of control over the polymerization process. Specifically, micropatterning reactions of intelligent polymer networks have been characterized allowing for the controlled integration as functional components of microdevices. Although a relatively slow reaction was analyzed in this study, the FTIR imaging methods can be utilized to capture an image for every several seconds. Therefore, the methods can be applied to much faster reactions. In addition, the scan time can be minimized by increasing the signal-to-noise ratio to decrease the number of scans needed. The novel characterization methods based on FTIR imaging presented within will facilitate the optimization of integration processes leading to enhanced (and reproducible) application of these and other intelligent materials as functional components in a wide variety of microdevices.

Acknowledgements

This research work was supported in part by a grant from the Kentucky Science and Engineering Foundation as per Grant Agreement #KSEF 799-RDE-007 with the Kentucky Science and Technology Corporation.

References

[1] Peppas NA, Hilt JZ, Khademhosseini A, Langer R. Adv Mater 2006;18:1345–60.
[2] Bashir R, Hilt JZ, Gupta A, Elibol O, Peppas NA. Appl Phys Lett 2002;81:3091–3.
[3] Hilt JZ, Gupta AK, Bashir R, Peppas NA. Biomed Microdevices 2003;5:177–84.
[4] Beebe DJ, Moore JS, Bauer JM, Yu Q, Liu RH, Devadoss C, et al. Nature 2000;404:588–90.
[5] Sershen SR, Mensing GA, Ng M, Halas NJ, Beebe DJ, West JL. Adv Mater 2005;17:1366–8.
[6] Peppas NA. Hydrogels in medicine and pharmacy. Boca Raton, FL: CRC Press; 1986.
[7] Hoffman AS. Adv Drug Delivery Rev 2002;54:3–12.
[8] Peppas NA, Huang Y, Torres-Lugo M, Ward JH, Zhang J. Ann Rev Biomed Eng 2000;2:9–29.
[9] Ehrick JD, Deo S, Browning TW, Bachas LG, Madou MJ, Daunert S. Nat Mater 2005;4:298–302.
[10] Hilt JZ, Byrne ME. Adv Drug Delivery Rev 2004;56:1599–620.
[11] Chan KLA, Kazarian SG. J Comb Chem 2005;7:185–9.
[12] Lewis EN, Treado PJ, Reeder RC, Story GM, Dowrey AE, Marcott C, et al. Anal Chem 1995;67:3377–81.
[13] Bhargava R, Wang S, Keonig JL. Adv Polym Sci 2003;163:137–91.
[14] Coutts-Lendon CA, Wright NA, Mieso EV, Keonig JL. J Controlled Release 2003;93:223–48.
[15] van der Weerd J, Kazarian SG. J Controlled Release 2004;98:295–305.
[16] Kazarian SG, Andrew Chan KL. Macromolecules 2003;36:9866–72.
[17] Fleming OS, Andrew Chan KL, Kazarian SG. Polymer 2006;47:4649–58.
[18] González-Benito J, Koenig JL. Polymer 2006;47:3065–72.
[19] Fernandez DC, Bhargava R, Hewitt SM, Levin IW. Nat Biotechnol 2005;23:469–74.
[20] Rafferty DW, Koenig JL, Magyar G, West JL. Appl Spectrosc 2002;56:1549–51.
[21] Kim B, Peppas NA. Polymer 2003;44:3701–7.
[22] Philippova OE, Karibyants NS, Stardubtzev SG. Macromolecules 1994;27:2398–401.
[23] Odian G. Principles of polymerization. 4th ed. NJ: Wiley; 2004.